

# Phase separation and mechanical responses of polyurethane nanocomposites

Junrong Zheng<sup>a,b,1</sup>, Rahmi Ozisik<sup>a,c,\*</sup>, Richard W. Siegel<sup>a,c</sup>

<sup>a</sup> Rensselaer Nanotechnology Center, Rensselaer Polytechnic Institute, 110 Eighth Street, Troy, NY 12180, USA

<sup>b</sup> Department of Chemistry, Rensselaer Polytechnic Institute, 110 Eighth Street, Troy, NY 12180, USA

<sup>c</sup> Department of Material Science and Engineering, Rensselaer Polytechnic Institute, MRC-205 110 Eighth Street, Troy, NY 12180, USA

Received 24 May 2006; received in revised form 19 August 2006; accepted 21 August 2006

Available online 25 September 2006

## Abstract

Nanocomposites of a diamine-cured polyurethane with nanofillers of different kinds, sizes, and surfaces were studied. Atomic force microscopy, scanning electron microscopy, X-ray diffraction, tensile tests, and dynamic mechanical thermal analysis were employed in the experiments. Experimental results suggest that mechanical properties are strongly correlated to polymer phase separation, which depends on the nature of the interface between the polymer and the nanoparticles. Two stages of phase separation were observed: the first stage involves the self-assembly of the hard segments into small hard phases of about 10 nm in width; the second stage involves the assembly of the 10 nm wide hard phases into larger domains of about 40–100 nm in width. In the case of polyurethane/ZnO nanocomposites with 5 wt% (less than 1 vol%) 33 nm ZnO nanoparticles, the covalent bonds that were formed between the polymer and ZnO surface hydroxyl groups constrain both stages of phase separation in polyurethane, resulting in approximately 40% decrease in the Young's modulus, 80% decrease in the strain at fracture, and 11 °C increase in the glass transition temperature of the soft segments. In the case of polyurethane/Al<sub>2</sub>O<sub>3</sub> nanocomposites with 5 wt% 15 nm Al<sub>2</sub>O<sub>3</sub> nanoparticles, hydrogen bonds between the particles and the polymer mainly constrain the second step of the phase separation, resulting in about 30% decrease in the Young's modulus and 12 °C increase in the glass transition temperature, but only a moderate decrease in the strain at fracture. The most striking results come from polyurethane/clay composites, where only van der Waals type interactions exist between polyurethane and the organically modified clay (Cloisite 20A). With the addition of 5 wt% surface modified clay (Cloisite 20A), both the Young's modulus and the strain at fracture decrease more than 80%, but the glass transition temperature increases by about 13 °C. Adding 10 wt% Cloisite 20A into polyurethane almost totally disrupts the phase separation, resulting in a very soft composite that resembles a "viscous liquid" rather than a solid.

© 2006 Elsevier Ltd. All rights reserved.

**Keywords:** Interfacial interactions; Glass transition; Mechanical properties

## 1. Introduction

In recent years polymer nanocomposites have attracted extensive interest around the world due to the many superior properties [1–5] they offer compared to traditional composites with micron-size fillers. One of the most important advantages

of nanocomposites over microcomposites is that the addition of a small amount of nanofillers (1–2 vol%) can change the mechanical properties of the composite dramatically [1,6]. Many polymer nanocomposites have been studied over the years [7–13]. As one of the most versatile polymers, polyurethane is among those that have been studied extensively. There have been more than 100 publications dealing with polyurethane nanocomposites since the publication of the first study in 1998 [6].

It is interesting to point out that, even for similar polyurethane systems and nanofillers (mainly surface modified clays), different groups have reported somewhat inconsistent findings. Wang and Pinnavaia [6], and Tien and Wei [14] reported an

\* Corresponding author. Department of Material Science and Engineering, Rensselaer Polytechnic Institute, MRC-205, 110 Eighth Street, Troy, NY 12180, USA.

E-mail address: [ozisik@rpi.edu](mailto:ozisik@rpi.edu) (R. Ozisik).

<sup>1</sup> Present address: Department of Chemistry, Stanford University, Stanford, CA 94305, USA.

increase both in the Young's modulus and the elongation, Zilg et al. reported an increase in the elongation, but a decrease in the Young's modulus [15], Han et al. reported a decrease in the elastic modulus and an increase in the elongation [16], while Xia et al. reported an increase in the modulus, but a decrease in the elongation as a result of exfoliation [17]. Our own experiments [8] showed even more surprising results: the addition of less than 1 vol% 33 nm ZnO induced a dramatic decrease in both the modulus and the elongation, but an obvious increase in the glass transition temperature of the soft segments in polyurethane. Our detailed measurements suggested that the phase separation of polyurethane is disrupted by reactions between the ZnO surface hydroxyl groups and the polymer, resulting in the observed unusual mechanical and thermal properties [8].

Two possible reasons exist that can explain the inconsistency in the literature regarding polyurethane/clay nanocomposites. First of all, the processing methods used to prepare the composites differed in these publications (either melt mixing or solution mixing was used). Different processing methods inevitably cause different filler distributions and exfoliation of the clay layers. Obtaining a good distribution of the filler is particularly challenging during melt mixing because of the short pot time and high viscosity of polyurethane. Secondly, both the polyurethanes and the clays used were different in most studies. Polyurethane is a well-known block copolymer, consisting of alternating soft and hard segments, which can self-assemble into two phases [18]. The phase separation is critical for the excellent mechanical properties of polyurethane [18]. These two differences can alter the phase separation and result in the observed inconsistent properties.

It is interesting that, except for our previous publication [8], no other studies have correlated the mechanical properties to the phase separation in polyurethane nanocomposites [6,14–17,19–25]. Based on small angle X-ray scattering and small angle neutron scattering data, Finnigan et al. believed that the phase separation was not disrupted by the addition of layered silicate nanofillers in their polyurethane system [25], though the increase in modulus was obvious. Han et al. observed a lower storage modulus and a higher soft segment glass transition temperature in the most exfoliated polyurethane/clay composite samples compared to neat polyurethane [16], similar to our observations in polyurethane/ZnO nanocomposites, but they did not give an explanation for their results. Recent molecular dynamic simulations by Zeng et al. showed that there was no obvious phase separation in polyurethane/clay composites between exfoliated clay layers because the van der Waals forces between the polyurethane polymer chains and the clay surface organic modifiers block the self-assembly of the polymer segments [26,27]. Based on their results, it is reasonable to assume that there can be no phase separation throughout the whole composite, if a suitable amount of clay is fully exfoliated in the polyurethane matrix, and as a result, the mechanical properties can drop sharply with the addition of the clays. This is similar to our observations in polyurethane/ZnO nanocomposites. To test our conclusions for the polyurethane/ZnO system (that the disruption of phase

separation is generally responsible for the mechanical changes) [8] and to further explore factors controlling the phase separation in the polyurethane nanocomposites, we extended our study to polyurethane composites with Al<sub>2</sub>O<sub>3</sub> nanoparticles of different sizes and surface modifications, and with clays with different surface modifications. In order to establish the connection between the interfacial interactions and phase separation in polyurethane, polyurethane/ZnO nanocomposite results will also be briefly described.

## 2. Experimental section

### 2.1. Sample preparation

The procedure used to prepare polyurethane composites was described in detail elsewhere [8] and is briefly described here as follows (all mixtures are by weight): equal molar ratios of a degassed polyurethane prepolymer (TDI-PPG prepolymer with brand name Airthane<sup>®</sup> PPT-95A from Air Products with 6.32 wt% NCO) and a diamine curative (aromatic diamine with brand name Lonzacure<sup>®</sup> MCDEA Curative from Air Products) were dissolved in purified THF to form a 15% solution at 25 °C. ZnO (33 nm average size from Nanophase Technologies Corporation; and 2.5 μm from Atlantic Equipment Engineers), Al<sub>2</sub>O<sub>3</sub> (15 nm from Nanotechnologies; 38 and 50 nm average size from Nanophase Technologies Corporation), or montmorillonite clay (Cloisite 20A and Cloisite 30B from Southern Clay products, used as received) was dispersed in THF with a sonicator to form a 10% solution. The two solutions were combined and sonicated for 20 min in an ice/water bath. Subsequently, the mixture was concentrated to a 60% solution. The solution was cast into molds and cured at 40 °C for 8 h and then cured at 110 °C for 24 h to form samples with thicknesses in the range of 0.2–3.0 mm. Neat polyurethane samples were prepared in the same way as the composites. In cured samples, the hard to soft segment ratio is ~0.35:1 by weight. The distribution of the fillers in the composites by the solution method described here is much better than the traditional melt mixing method [8].

### 2.2. Atomic force microscopy (AFM)

Atomic force microscopy (MultiMode Scanning Probe Microscope from Digital Instruments) measurements were conducted at room temperature using the tapping mode. The samples analyzed were neat polyurethane and composites with two different film thickness values: ~500 μm (bulk, prepared from 60% THF solution) and <1 μm (thin film, prepared from 10% THF solution by spin coating at 3000 rpm on silicon wafers).

### 2.3. Field emission scanning electron microscopy (FE-SEM)

Fractographs were observed with an FE-SEM (JEOL JSM-6330F). Samples were prepared by tearing prenotched samples (~0.5 mm thick) at room temperature (~21 °C). All samples

were coated with a layer of gold or platinum before SEM characterization.

#### 2.4. Dynamic mechanical thermal analysis (DMTA) and tensile tests

The mechanical responses of samples were measured with a DMTA (DMTA V, Rheometric Scientific) and an Instron 8562. Two kinds of DMTA measurements (both at 1 Hz) were performed: (i) dynamic strain sweep at room temperature ( $\sim 21^\circ\text{C}$ ), giving the storage modulus, and (ii) dynamic temperature ramp sweep at 0.1% strain and  $2^\circ\text{C}/\text{min}$  from  $-130^\circ\text{C}$  to  $200^\circ\text{C}$ , giving the glass transition temperature of the soft segments and the loss factor. The DMTA experiments were performed using a tensile test fixture.

Tensile tests were performed to obtain the Young's modulus and the strain at fracture at room temperature at a rate of 10 mm/min. The neck dimension of the samples was  $2.7 \times 2.8 \times 13$  mm. Each data point is averaged from three to six samples.

### 3. Results and discussion

#### 3.1. Polyurethane/ZnO nanocomposites

ZnO nanoparticles have a very special property in that they have no detectable surface water compared to other metal oxide nanoparticles, such as  $\text{Al}_2\text{O}_3$ ,  $\text{TiO}_2$ , and  $\text{SiO}_2$ . This characteristic enables ZnO nanoparticles to induce crystallization of Nylon 6 on the particles' surface [7] and to react with the isocyanate groups of the polyurethane prepolymer [8]. Because of the reaction between the isocyanate groups of the polyurethane prepolymer and ZnO, the mechanical behavior of the polyurethane/ZnO nanocomposites is quite unique. Detailed studies on the nanocomposites of polyurethane with ZnO particles of different sizes and surfaces have been reported in our previous publication [8]. A brief description of the results will be presented in the following paragraphs. Some of the data are listed in Table 1.

With the addition of 5% ( $\sim 1$  vol%) 33 nm ZnO nanoparticles into polyurethane (polymer/particle interfacial area is about  $200\text{ m}^2/100\text{ g}$  of composite), the Young's modulus, storage modulus and strain at fracture of the composite decreased approximately 38, 52, and 80%, respectively, while the soft segment glass transition temperature ( $T_g$ ) increased  $\sim 11^\circ\text{C}$  compared to the neat polyurethane. These changes were attributed to the disruption of the phase separation by the addition of the ZnO nanoparticles. The origin of the disruption is the reaction between the polyurethane and the surface hydroxyl groups on the particles [8]. The high modulus and large strain at fracture of the polyurethane are related to the phase separation of the hard and soft segments [18]. Therefore, it is reasonable to propose that a disruption of the phase separation in the polyurethane nanocomposites results in the observed decrease both in the modulus and strain at fracture. The increased  $T_g$  results from constraints induced by the interfacial reactions.

AFM measurements suggested that there are two stages of phase separation in the polyurethane used in this study. The first stage involves the self-assembly of the hard segments into small hard phases of about 10 nm in width, which is similar to the observations of McLean and Sauer [28]. The second stage involves the assembly of the 10 nm wide hard phases into larger domains of about 40–100 nm in width. In the polyurethane/ZnO nanocomposites, both stages of the phase separation in polyurethane were disrupted by the addition of nanoparticles. Fig. 1 shows the AFM phase images of (a) neat bulk polyurethane and (b) nanocomposite with 5% 33 nm ZnO bulk samples. The two length scales associated with the two stages of phase separation are clearly observed in Fig. 1a, whereas Fig. 1b does not show the two length scales. FE-SEM measurements supported the AFM findings. Fig. 2 shows fracture surfaces of (a) the neat polyurethane and (b) polyurethane nanocomposite with 5% 33 nm ZnO fractured at room temperature (above the  $T_g$  of the soft segments). The neat polyurethane has a smooth surface, whereas the nanocomposite has a very rough surface. This difference in surface roughness can result from the following reasons. After fracture, a layer of soft phase rearranges to cover the surface of

Table 1  
Results of the tensile tests and dynamic mechanical thermal analysis (DMTA)

| Sample                                     | $T_g$ ( $^\circ\text{C}$ ) | Loss factor | $G'^a$ (MPa) | $E^a$ (MPa)    | Strain at fracture |
|--|----------------------------|-------------|--------------|----------------|--------------------|
| Polyurethane                               | -2.9                       | 0.18        | 19.6         | $38.3 \pm 2$   | $7.5 \pm 1.0$      |
| 5 wt% 33 nm ZnO                            | 8.3                        | 0.30        | 9.3          | $23.9 \pm 0.7$ | $1.16 \pm 0.2$     |
| 5 wt% 15 nm $\text{Al}_2\text{O}_3$        | 9.4                        | 0.23        | 12.0         | $26.0 \pm 1$   | $4.6 \pm 0.8$      |
| 5 wt% 38 nm $\text{Al}_2\text{O}_3$        | 2.0                        | 0.18        | 17.0         | $37.2 \pm 2$   | $4.9 \pm 1$        |
| 5 wt% 50 nm $\text{Al}_2\text{O}_3$        | -2.0                       | 0.18        | 17.8         | $38.3 \pm 2$   | $4.8 \pm 0.8$      |
| 5 wt% 15 nm $\text{Al}_2\text{O}_3$ (Si-1) | -10.0                      | 0.17        | 21.1         | $43.5 \pm 2$   | $4.8 \pm 1$        |
| 5 wt% 15 nm $\text{Al}_2\text{O}_3$ (Si-2) | -2.3                       | 0.18        | 20.0         | $37.6 \pm 2$   | $5.1 \pm 1$        |
| 2 wt% Clay 20A                             | 12.1                       | 0.28        | 10           | $18.8 \pm 1$   | $3.1 \pm 0.6$      |
| 5 wt% Clay 20A                             | 10.0                       | 0.39        | 5.4          | $7.6 \pm 0.4$  | $1 \pm 0.1$        |
| 10 wt% Clay 20A                            | —                          | —           | <2.2         | <3.8           | <0.3               |
| 2 wt% Clay 30B                             | 8.6                        | 0.24        | 13           | $23.3 \pm 1$   | $4.2 \pm 1$        |
| 5 wt% Clay 30B                             | 10                         | 0.30        | 10.6         | $19.1 \pm 1$   | $1.6 \pm 0.3$      |
| 10 wt% Clay 30B                            | 10                         | 0.49        | <5.6         | <4.7           | $0.4 \pm 0.4$      |

The dynamic mechanical tests were performed at a frequency of 1 Hz and 0.1% strain.

<sup>a</sup> The modulus values were exaggerated by a factor of 10 times in our previous publication [8] due to a unit error.

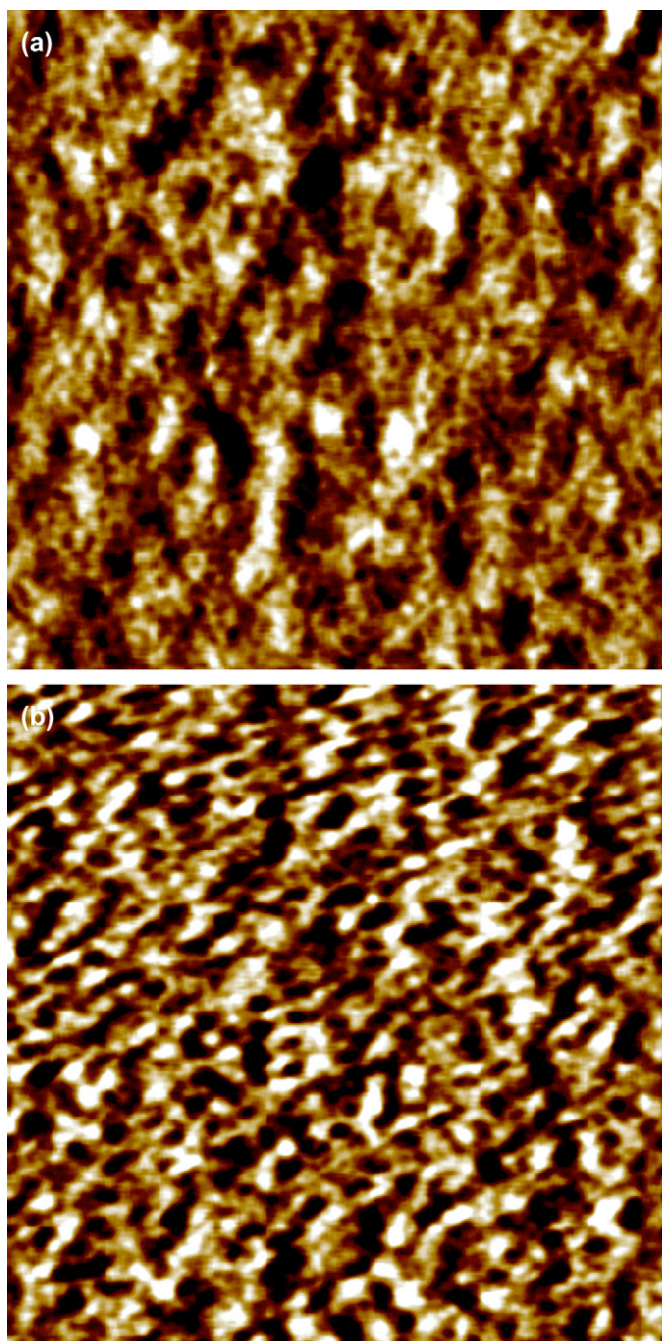


Fig. 1. AFM phase images for (a) neat bulk polyurethane (with maximum  $z$ -axis scale of  $1.7^\circ$ ) and (b) polyurethane composite bulk sample with 5% 33 nm ZnO nanoparticles (with maximum  $z$ -axis scale of  $2^\circ$ ). Image size is  $1 \times 1 \mu\text{m}$ .

the neat polyurethane because the soft phase has a lower surface energy and a low  $T_g$  [28]. This soft-phase surface layer creates a smooth surface to minimize the surface area. In the nanocomposite, the soft phase cannot efficiently cover the surface because of poor phase separation and, most importantly, it is constrained by the interfacial interactions between the polymer and the nanoparticles (as deduced from the increase in  $T_g$ ). Surface modification of the ZnO nanoparticles and FTIR measurements [8] confirmed that the interfacial reaction

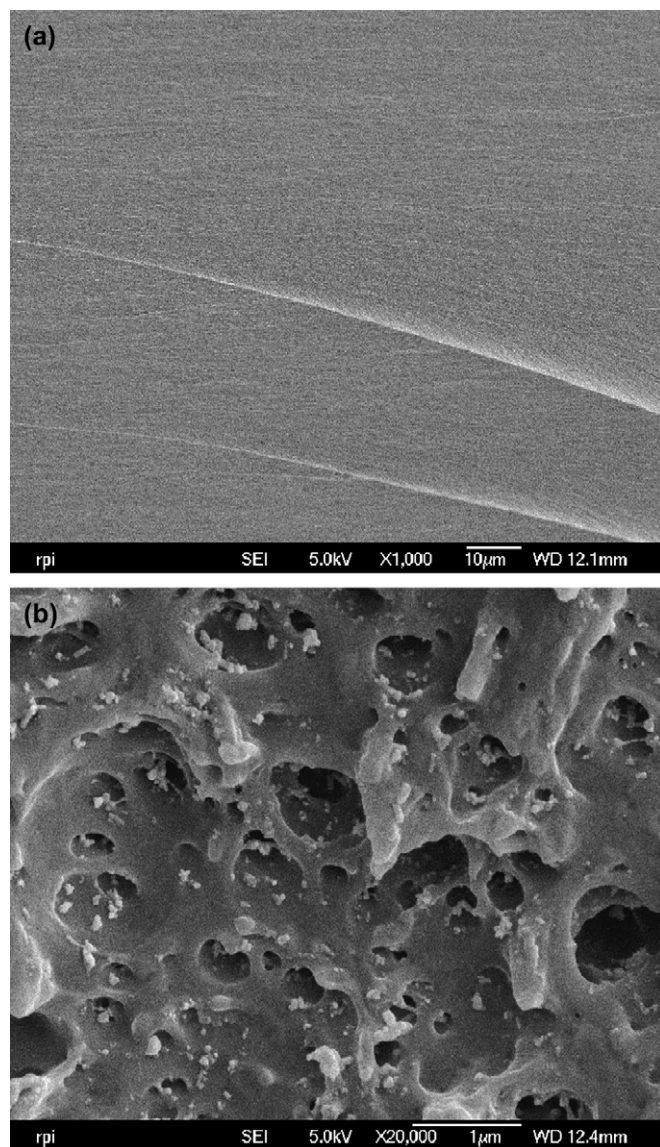


Fig. 2. SEM fractographs of (a) neat polyurethane and (b) polyurethane composite sample with 5% 33 nm ZnO nanoparticles fractured at room temperature.

between the nanoparticles and polyurethane is a key reason for the disruption of phase separation in the nanocomposite system. The disruption of the phase separation can be controlled by modifying the surface of ZnO nanoparticles as shown by our previous work [8].

### 3.2. Polyurethane/ $\text{Al}_2\text{O}_3$ nanocomposites

The surface chemistry of  $\text{Al}_2\text{O}_3$  nanoparticles is different from that of ZnO nanoparticles.  $\text{Al}_2\text{O}_3$  nanoparticles have surface water that is particle size dependent. When measured with TGA, 15, 38 and 50 nm  $\text{Al}_2\text{O}_3$  particles have 4.5, 1.5 and 0.8 wt% surface water, respectively. The mechanical properties of polyurethane/ $\text{Al}_2\text{O}_3$  nanocomposites are also quite different from those of polyurethane/ZnO nanocomposites. The Young's and storage moduli of the nanocomposite with 5%

38 nm  $\text{Al}_2\text{O}_3$  are only about 5–10% smaller compared to neat polyurethane (38 nm  $\text{Al}_2\text{O}_3$  and 33 nm ZnO have similar surface areas, the density of  $\text{Al}_2\text{O}_3$  is 3.6 g/cm<sup>3</sup> and the density of ZnO is 5.6 g/cm<sup>3</sup>). The strain at fracture of the  $\text{Al}_2\text{O}_3$  nanocomposite is about 30% lower and the  $T_g$  of the soft segments in the  $\text{Al}_2\text{O}_3$  nanocomposite is about 4 °C higher than the  $T_g$  of the neat polyurethane. The decrease in strain at fracture is probably due to the interfacial defects induced by adding the fillers; adding a similar amount of micron-size fillers yields a similar result. The trend of the mechanical responses in the polyurethane/ $\text{Al}_2\text{O}_3$  nanocomposites is similar to that in the polyurethane/ZnO nanocomposites, but the magnitude of change is smaller. When 50 nm  $\text{Al}_2\text{O}_3$  nanoparticles were used, the mechanical properties of the 5% nanocomposite were almost the same as those of the neat polyurethane. Detailed data are listed in Table 1.

The mechanical changes in the polyurethane composite with 5% 15 nm  $\text{Al}_2\text{O}_3$  nanoparticles ( $\sim 1.5$  vol%, and polymer/particle interfacial area is about 500 m<sup>2</sup>/100 g of composite) are more apparent than for the two larger  $\text{Al}_2\text{O}_3$  nanoparticles (38 and 50 nm). Both the Young's and storage moduli decreased by about 35%, and the  $T_g$  of the soft segments increased about 12 °C compared to the neat polyurethane. These values are similar to those of the nanocomposite with 5% 33 nm ZnO. The strain at fracture of the 15 nm  $\text{Al}_2\text{O}_3$  composite is still close to that of the neat polyurethane (which is about 500%) and is quite different from that of the ZnO nanocomposite (which is about 100%). The difference in the strain at fracture between the two nanocomposites might be due to their different microstructures.

Fig. 3 shows AFM phase images of (a) a neat polyurethane thin film, and (b) the nanocomposite bulk sample with 5% 15 nm  $\text{Al}_2\text{O}_3$ . The images of the polyurethane/ $\text{Al}_2\text{O}_3$  (Fig. 3b) and the polyurethane/ZnO nanocomposites (Fig. 1b) are quite different. The small length scale domains associated with the first stage of phase separation (the formation of 10 nm wide domains) can be clearly observed in the polyurethane/ $\text{Al}_2\text{O}_3$  nanocomposite, but the 40–100 nm domains (that are associated with the second stage of phase separation) are not obvious, compared to the neat bulk polyurethane (Fig. 1a). The bulk morphology of the polyurethane/ $\text{Al}_2\text{O}_3$  nanocomposite is almost like an “intermediate state” between the neat bulk polyurethane (Fig. 1a) and the polyurethane thin film (Fig. 3a). The average size of the hard phases in the  $\text{Al}_2\text{O}_3$  nanocomposite is smaller than that in the bulk polyurethane, but obviously larger than that in the polyurethane thin film. Larger domains are present in the bulk polyurethane, but not in the thin film, and a small amount is observed in the polyurethane/ $\text{Al}_2\text{O}_3$  composite. Polyurethane thin films have a lower modulus than the bulk polyurethane, but the strain at fracture is not severely affected. The results seem to suggest that the second step of the phase separation is mainly responsible for the modulus, and the first step is responsible for both the modulus and strain at fracture.

SEM measurements also suggested a difference in the morphologies of the polyurethane/ $\text{Al}_2\text{O}_3$  and polyurethane/ZnO composites. Fig. 4a and b is fracture surfaces of polyurethane composites with 5%, 15 and 50 nm  $\text{Al}_2\text{O}_3$  nanoparticles,

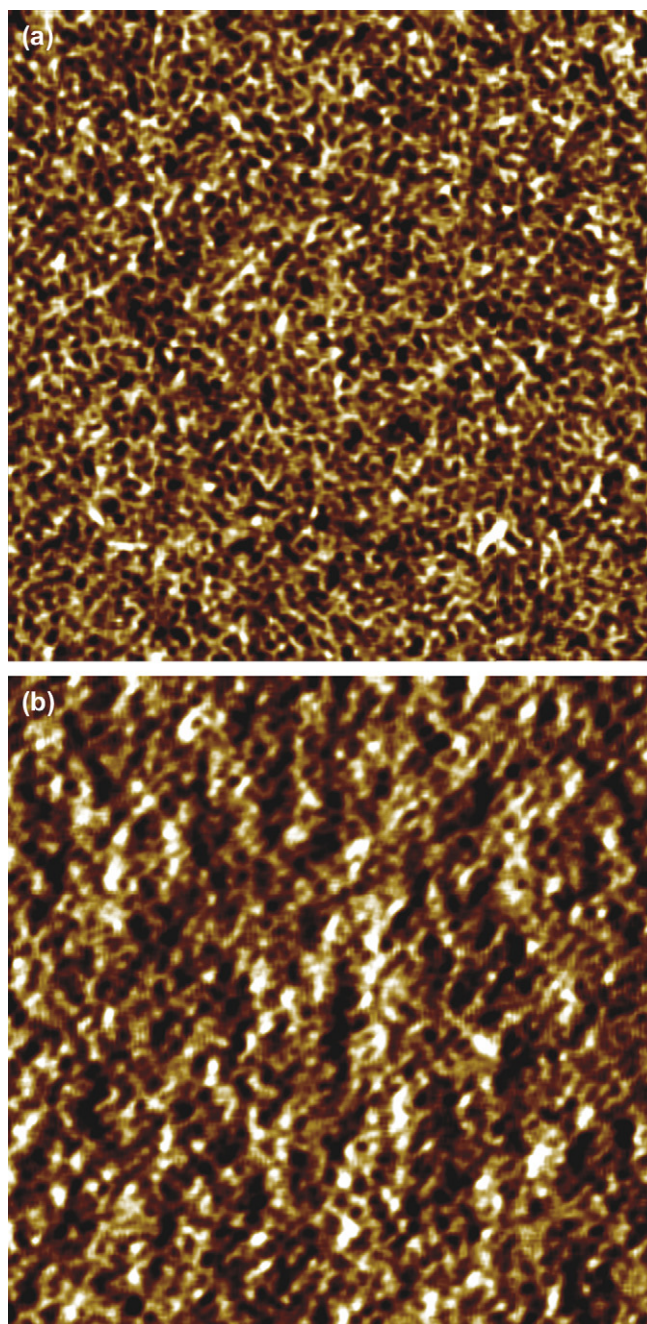


Fig. 3. AFM images for (a) polyurethane thin film (with maximum z-axis scale of 6°) and (b) polyurethane composite bulk sample with 5% 15 nm  $\text{Al}_2\text{O}_3$  nanoparticles polyurethane (with maximum z-axis scale of 3°). Image size is 1 × 1 μm.

respectively. Both of these images are quite different from the polyurethane/ZnO nanocomposite (Fig. 2b). The fracture surface of the composite with 50 nm  $\text{Al}_2\text{O}_3$  particles is very smooth (Fig. 4b), which is similar to what we observed for the polyurethane/ZnO microcomposite [8]. Following the explanation given for polyurethane/ZnO in the previous section, we can deduce that the phase separation of polyurethane is rarely disrupted in the composite with 50 nm  $\text{Al}_2\text{O}_3$  particles. The composite with 15 nm  $\text{Al}_2\text{O}_3$  particles has a rougher fracture surface (Fig. 4a) than the composite with 50 nm  $\text{Al}_2\text{O}_3$

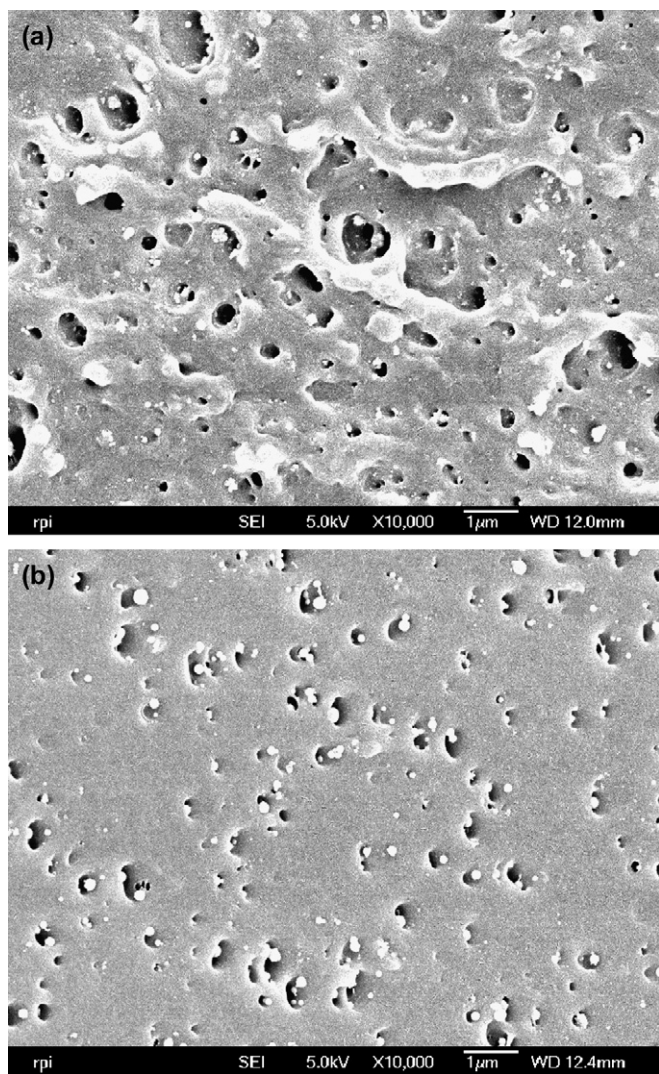


Fig. 4. SEM fractographs of polyurethane composite samples with 5% (a) 15 nm and (b) 50 nm  $\text{Al}_2\text{O}_3$  nanoparticles fractured at room temperature.

particles, but still much smoother than the polyurethane/ $\text{ZnO}$  composite (Fig. 2b). The results imply that the phase separation is somehow disrupted in the composite with 15 nm  $\text{Al}_2\text{O}_3$  particles, but that the disruption is not as severe as in the polyurethane/ $\text{ZnO}$  nanocomposite. The SEM measurements were consistent with the mechanical and AFM measurements described above.

The mechanical responses of the 15 nm polyurethane/ $\text{Al}_2\text{O}_3$  composite can be tuned by modifying the surfaces of the  $\text{Al}_2\text{O}_3$  particles. Two kinds of silanes were used in the surface modification to create two very different situations. In the first case (Si-1 with the chemical formula  $(\text{C}_2\text{H}_5\text{O})_3\text{Si}(\text{CH}_2)_3\text{NH}(\text{CH}_2)_2\text{NH}_2$ ), the silane has amine groups that can react with the polyurethane prepolymer so that the nanoparticles can be chemically tethered to the polymer chains. The second silane (Si-2 with the chemical formula  $\text{Cl}(\text{CH}_3)_2\text{Si}(\text{CH}_2)_9\text{CH}_3$ ) does not react with the polyurethane prepolymer. As expected, the mechanical properties of the polyurethane composite with 5% 15 nm  $\text{Al}_2\text{O}_3$  particles coated

with Si-2 are the same as the neat polymer, because the coating prevents the interactions between the polymer and the particles (see Table 1 and Fig. 5). Interestingly, the sample with 5% 15 nm  $\text{Al}_2\text{O}_3$  particles coated with Si-1 has greater Young's and storage moduli ( $\sim 10\%$  higher) and lower  $T_g$  ( $\sim 7^\circ\text{C}$  lower) than the neat polyurethane. These results are opposite to what we observed for the composites with uncoated  $\text{Al}_2\text{O}_3$  and  $\text{ZnO}$  nanoparticles. It seems that the relationship between the microstructure and the interfacial interactions is much more complicated than what we have imagined. On the other hand, these results point out the possibility that the properties of the polymer can be controlled by changing the interactions between the nanoparticles and the polymer. Fig. 5 shows the temperature dependent loss factors for the neat polyurethane and the polyurethane/ $\text{Al}_2\text{O}_3$  composites with 5% loading. The peak position represents the glass transition temperature of the soft segments and the samples with weaker elasticity show greater peak intensity. The composites with 15 nm  $\text{Al}_2\text{O}_3$  nanoparticles uncoated and coated with Si-1 are obviously different from the other samples. The composite with uncoated 15 nm  $\text{Al}_2\text{O}_3$  nanoparticles yields the highest  $T_g$  and the poorest elasticity, while the composite with Si-1 coated particles shows the lowest  $T_g$  and the best elasticity.

The above results indicate that the interfacial interactions between the 15 nm  $\text{Al}_2\text{O}_3$  particles and the polyurethane are critical for the mechanical responses. The polymer and  $\text{Al}_2\text{O}_3$  particles are bound by hydrogen bonds (the surface water is loosely bound to the  $\text{Al}_2\text{O}_3$  particles by hydrogen bonds). The hydrogen bonds are much weaker and more flexible than the covalent bonds between the polyurethane and  $\text{ZnO}$  nanoparticles. Therefore, the extent of the disruption of phase separation in polyurethane/ $\text{Al}_2\text{O}_3$  composites is not as severe as it is in the polyurethane/ $\text{ZnO}$  nanocomposites. Similar size  $\text{ZnO}$  and  $\text{Al}_2\text{O}_3$  nanoparticles have different effects on the polyurethane because of the differences in their interfacial interactions. On the other hand, 15 nm  $\text{Al}_2\text{O}_3$  nanoparticles ( $\sim 100\text{ m}^2/\text{g}$ ) have

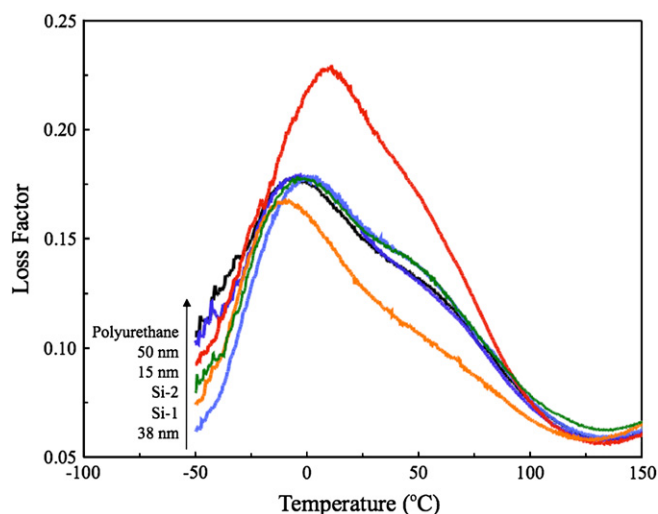


Fig. 5. Loss factors ( $\tan \delta$ ) of polyurethane/ $\text{Al}_2\text{O}_3$  (5%) nanocomposites as a function of temperature compared to neat polyurethane obtained by DMTA dynamic temperature sweep measurements.

similar effects on polyurethane to 33 nm ZnO nanoparticles ( $\sim 40 \text{ m}^2/\text{g}$ ) because of their larger surface area.

### 3.3. Polyurethane/clay nanocomposites

The montmorillonite clays are known to have a very large surface area ( $\sim 760 \text{ m}^2/\text{g}$ ) compared to  $\text{Al}_2\text{O}_3$  and ZnO nanoparticles. If one can fully exfoliate clay layers in polyurethane, greater mechanical changes might then be realized. In the current study, two types of clays with different surface chemistries were chosen for comparison: Cloisite 20A and Cloisite 30B. Cloisite 20A is covered by a layer of about 38% organic modifiers and the alkyl groups of the modifiers can form van der Waals interactions with polyurethane soft segments. Cloisite 30B, on the other hand, is covered by a layer of about 30% organic modifiers that include functional groups that can react with the polyurethane prepolymer.

The trend of the mechanical responses of polyurethane composites with 5% Cloisite 20A and Cloisite 30B is similar to those of polyurethane/ZnO nanocomposites. The Young's and storage moduli of the composite with 5% 20A ( $\sim 3 \text{ vol}\%$ , the polymer/particle interfacial area is about  $3800 \text{ m}^2/100 \text{ g}$  of composite, if the clay is fully exfoliated) decreased about 80 and 85%, respectively, compared to the neat polyurethane. These values are lower than those of the polyurethane/ZnO nanocomposites. The  $T_g$  increased about  $13^\circ\text{C}$  compared to neat polyurethane. More surprisingly, adding 10% 20A into polyurethane results in a very soft composite, more like a viscous liquid rather than a solid. The properties of the composite with 5% 30B did not change as much as those of the 5% 20A composite. The Young's and storage moduli decreased about 50% and the  $T_g$  increased about  $13^\circ\text{C}$  compared to neat polyurethane (see Table 1). The composite with 10% 30B was also very soft. The possible reasons for the observed differences between the two clay composites are as follows: (i) the exfoliation is greater for Cloisite 20A and (ii) Cloisite 30B is chemically bonded to the polymer chains.

Fig. 6 shows the wide angle X-ray diffraction (WAXD) spectra of the two modified clay particles (Fig. 6a) and the polyurethane composites with 5% clay loading (Fig. 6b). The first peak position provides the gallery spacing between clay layers: 1.83 and 2.48 nm for 30B and 20A, respectively. There is a peak at around  $2.2^\circ$  in Fig. 6b for the 30B composite, indicating that some of the 30B clay layers did not exfoliate. The 20A composite does not have such a peak. The results suggest that the exfoliation is greater for 20A than 30B in polyurethane, even though 30B can react with the polyurethane prepolymer.

Based on the explanations given for the polyurethane/ZnO and polyurethane/ $\text{Al}_2\text{O}_3$  composites, we can deduce that the polymer phase separation in the 20A clay composite is disrupted more severely than in the ZnO composite, which means that the total interactions are stronger in the 20A composite because the mechanical property changes are greater in the 20A composite. The only interactions between the polymer and the 20A clay are the van der Waals forces between the

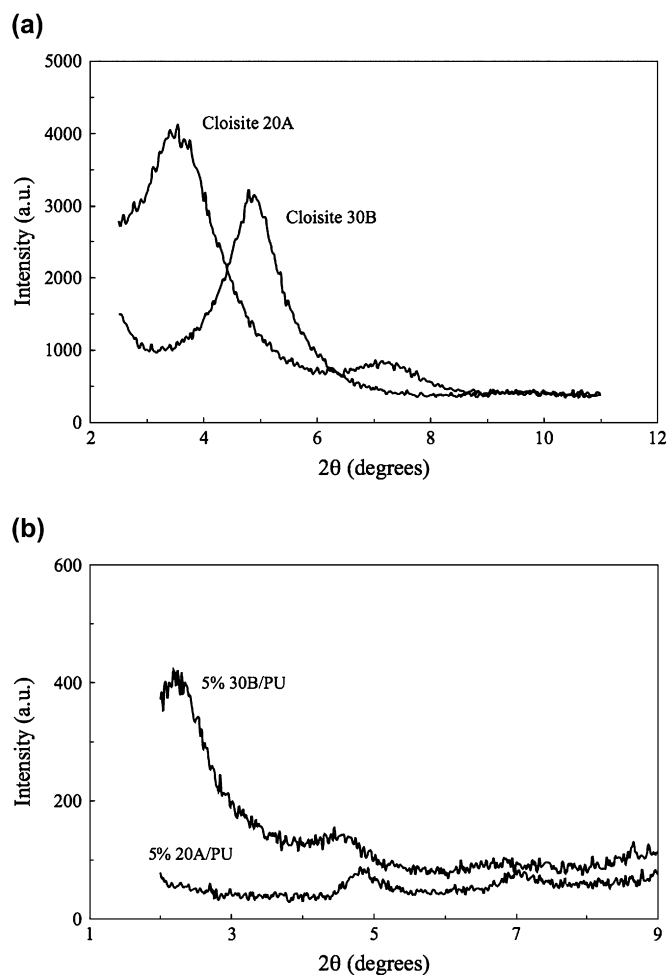


Fig. 6. Wide angle X-ray diffraction spectra for (a) pure clay particles and (b) 5% clay/polyurethane nanocomposites.

clay surface alkyl groups and the polymer chains, whereas the interactions between ZnO nanoparticles and polyurethane are stronger covalent bonds. To explain the mechanical results observed, the number of van der Waals interactions between the clay and polyurethane in the 20A composite must be much larger than that of the covalent bonds between the ZnO nanoparticles and polyurethane so that the total interfacial interactions are stronger.

AFM measurements on clay composites were unsuccessful because of the high roughness of the composite surfaces, which is quite different from the polyurethane/ZnO composite. In the polyurethane/ZnO composite, although the phase separation is severely disrupted, the sample surface is still covered with a thin layer of smooth soft phase. It seemed that even this surface layer was disrupted by the addition of 20A and 30B in the clay composites. Fig. 7 is an AFM topographic image of polyurethane composite with 2% Cloisite 20A. It can be seen that there are many clay layers on the surface.

SEM measurements provided some indirect information about the polymer phase separation in the 20A and 30B composites. Fig. 8 shows the fracture surfaces of polyurethane composites with 5% Cloisite 20A (Fig. 8a) and Cloisite 30B

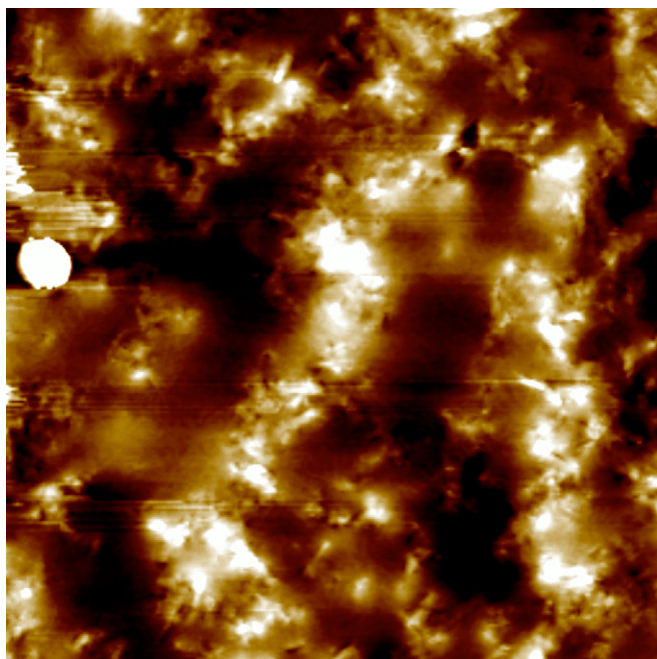


Fig. 7. AFM topograph of a 2% Cloisite 20A/polyurethane composite sample (maximum z-axis scale is 50 nm).

(Fig. 8b). The images are totally different from those of polyurethane/ZnO and polyurethane/ $\text{Al}_2\text{O}_3$  composites. The fracture surface is full of clay layers, but phase domains, which are obvious in polyurethane/ZnO and polyurethane/ $\text{Al}_2\text{O}_3$  composites, can hardly be seen in both Figs. 8a and b. These images suggest that the self-assembly process is severely constrained due to the presence of the clay particles. The results are consistent with the mechanical tests. The disruption of phase separation results in decreased modulus and strain at fracture. On the other hand, the  $T_g$  increases because of constraints imposed by the clay particles [29,30]. It is interesting to point out that  $T_g$  is larger in the 2% 20A composite than in the 5% composite. This may be due to the competing constraining effects of the phase separation and the clay layers, since the loss factor value for the 2% sample is obviously smaller.

These experimental results support the conclusion that there is no obvious phase separation in the polyurethane/20A composite. This conclusion seems strange, but it is reasonable. The interactions between 20A and polyurethane comprises van der Waals forces only. If the number of the van der Waals interactions is sufficiently large, in principle, the phase separation can be blocked (Si-2 coated  $\text{Al}_2\text{O}_3$  nanoparticles have weaker effects on polyurethane than Cloisite 20A because of smaller surface area), because the nature of the driving forces for the phase separation is also van der Waals forces. By molecular dynamic simulations, Zeng et al. demonstrated that the van der Waals forces between nonpolar alkyl chains of the modified clay and the soft segments of the polyurethane dominate the interactions between the organoclay and polyurethane [26,27]. Because of these interactions, there are no distinct phase-separated structures in polyurethane. These

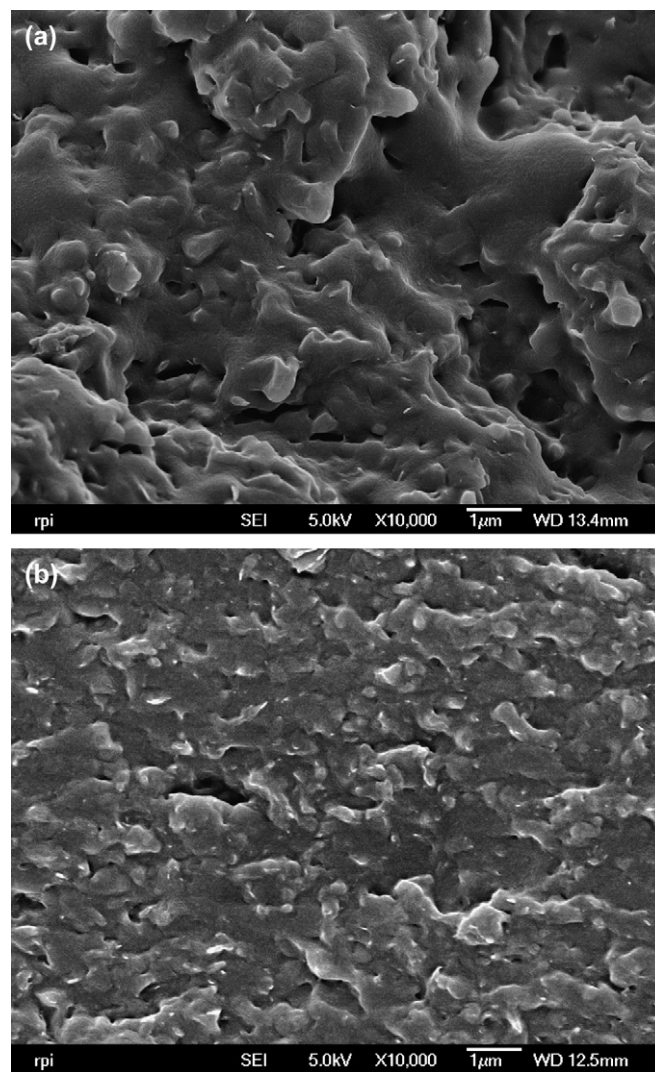


Fig. 8. SEM fractographs of polyurethane composite samples with 5% (a) Cloisite 20A and (b) Cloisite 30B clays fractured at room temperature.

simulation results are quite similar to the experimental findings of both the present study and our previous findings published in 2003 [31].

#### 4. Concluding remarks

The following conclusions are based on our observations involving three different nano-size particles.

- (1) The phase separation in polyurethane can be disrupted by the addition of a small amount of nano-size fillers. The disruption depends strongly on the interface and, therefore, can be controlled through surface modification of the nanoparticles.
- (2) The effect of disruption depends on the nature of the interfacial interaction, but most importantly on the extent of the interaction strength. It is important to note that it is the overall interaction strength, but not the strength of the individual interactions, that is important. This is why the



disruption of phase separation is observed in all possible cases (with different bonds), even in the case of weak van der Waals interactions.

- (3) The disruption of phase separation weakens the mechanical properties. However, the mechanical properties can be recovered, and in some cases improved, by chemically modifying the surfaces of the nanoparticles.
- (4) The glass transition temperature of the soft segments also changes as a result of interfacial interactions.

## Acknowledgements

Financial support from Albany International Corporation and the Nanoscale Science and Engineering Initiative of the National Science Foundation under NSF Award Number DMR-0117702 is gratefully acknowledged.

## References

- [1] Kojima Y, Usuki A, Kawasumi M, Okada O, Fukushima Y, Kurachi T, et al. *J Mater Res* 1993;8:1185.
- [2] Alexander M, Dubois P. *Mater Sci Eng Rev* 2000;28:1.
- [3] Balazs AC. *Curr Opin Colloid Interface Sci* 2000;4:443.
- [4] Giannelis EP. *Appl Organomet Chem* 1998;12:675.
- [5] Soo PP, Huang BY, Jang YI, Chiang YM, Sadoway DR, Mayers AM. *J Electrochem Soc* 1999;146:32.
- [6] Wang Z, Pinnavaia TJ. *Chem Mater* 1998;10:3769.
- [7] Zheng J, Siegel RW, Toney CG. *J Polym Sci Part B Polym Phys* 2003;41:1033.
- [8] Zheng J, Ozisik R, Siegel RW. *Polymer* 2005;46:10873.
- [9] Messersmith PB, Giannelis EP. *Chem Mater* 1994;6:1719.
- [10] Huang XY, Brittain WJ. *Macromolecules* 2001;34:3255.
- [11] Okamoto M, Morita S, Taguchi H, Kim YH, Kotaka T, Tateyama H. *Polymer* 2000;41:3887.
- [12] Yoon PJ, Hunter DL, Paul DR. *Polymer* 2003;44:5323.
- [13] Giri AK. *J Appl Phys* 1997;81:1348.
- [14] Tien YI, Wei KH. *Macromolecules* 2001;34:9045.
- [15] Zilg C, Thomann R, Mulhaupt R, Finter J. *Adv Mater* 1999;11:49.
- [16] Han B, Cheng A, Ji G, Wu S, Shen J. *J Appl Polym Sci* 2003;91:2536.
- [17] Xia H, Shaw SJ, Song M. *Polym Int* 2005;54:1392.
- [18] Hepburn C. *Polyurethane elastomers*. Essex, England: Elsevier Science; 1992.
- [19] Song M, Hourston DJ, Yao KJ, Tay JKH, Ansarifard MA. *J Appl Polym Sci* 2003;90:3239.
- [20] Dai X, Xu J, Guo X, Liu Y, Shen D, Zhao N, et al. *Macromolecules* 2004;37:5615.
- [21] Tien YI, Wei KH. *J Appl Polym Sci* 2002;86:1741.
- [22] Pattanayak A, Jana SC. *Polymer* 2005;46:3394.
- [23] Chen YC, Zhou SX, Yang HH, Wu LM. *J Appl Polym Sci* 2005;95:1032.
- [24] Kuan HC, Ma CCM, Chuang WP, Su HY. *J Polym Sci Part B Polym Phys* 2005;43:1.
- [25] Finnigan B, Martin D, Halley P, Truss R, Campbell K. *Polymer* 2004;45:2249.
- [26] Zeng QH, Yu AB, Lu GQ, Standish RK. *J Mater Sci Technol* 2005;21(Suppl. 1):114.
- [27] Zeng QH, Yu AB, Lu GQ. *Nanotechnology* 2005;16:2757.
- [28] McLean RS, Sauer BB. *Macromolecules* 1997;30:8314.
- [29] Zhao Q, Samulski ET. *Macromolecules* 2005;38:7967.
- [30] Agag T, Koga T, Takeichi T. *Polymer* 2001;42:3399.
- [31] Zheng, J. *Polymer/nanoparticle nanocomposites* MS Thesis, Rensselaer Polytechnic Institute, 2003.